Facchinetti, Irene ; Cobani, Elkid ; Brogioli, Doriano ; La Mantia, Fabio ; Ruffo, Riccardo

⊞

Thermally Regenerable Redox Flow Battery

Recommended Citation (primary publication/Version of Record) incl. DOI:

I. Facchinetti, E. Cobani, D. Brogioli, F. La Mantia, R. Ruffo. Thermally Regenerable Redox Flow Battery.
ChemSusChem 2020, 13 (20), 5460-5467. https://doi.org/10.1002/cssc.202001799

Take down policy
If you believe that this document or any material on this site infringes copyright, please contact
publizieren@suub.uni-bremen.de with full details and we will remove access to the material.

FULL PAPER

Thermally regenerable redox flow battery

Irene Facchinetti[a], Elkid Cobani[a], Doriano Brogioli[b], Fabio La Mantia[b] and Riccardo Ruffo*[a]

[a]   I. Facchinetti, Dr. E. Cobani, Prof. R. Ruffo
       Dipartimento di Scienze dei Materiali
       Università degli Studi di Milano Bicocca
       Via Cozzi, 55, Milano, 20125, Italy
       riccardo.ruffo@unimib.it

[b]   Dr. D. Brogioli, Prof. F. La Mantia
       Energiespeicher- und Energiewandlersysteme
       Universität Bremen
       Bibliothekstraße, 1, Bremen, 28359, Germany

       Supporting information for this article is given via a link at the end of the document.

Abstract: The efficient production of energy from low temperature heat sources (below 100°C) would open the doors to the exploitation of a huge amount of heat sources such as solar, geothermal and industrial waste heat. Thermal Regenerable Redox-Flow Batteries are flow batteries that store energy in concentration cells which can be recharged by distillation at temperature <100°C, exploiting low temperature heat sources. Using a single membrane cell set-up and a proper redox couple ($LiBr/Br_2$), we have developed a Thermal Regenerable Redox-Flow Battery (TRB) able to store a maximum volumetric energy of 25.5 Wh dm^{-3}, which can be delivered at power density of 8 W m^{-2}. After discharging the 30% of the volumetric energy, a total heat to electrical energy conversion efficiency of 4% is calculated, the highest value reported so far in harvesting of low-temperature heat.

Introduction

Globally, 60% of the primary produced energy is lost as low-temperature heat (<100°C, LTH)[1,2]. The harvesting of wasted heat and other natural thermal sources *e.g.* geothermal heat, solar heat and cogeneration plants, would lead to a significant improvement in the exploitation of world energy resources and a more efficient energy production, reducing their environmental impact[3,4]. At present day, there are no commercial systems that can harvest this type of energy, reaching satisfactory heat conversion efficiency at an affordable price. Different devices have been proposed, e.g. Organic Rankine Cycle (ORC)[5] and

solid-state thermoelectric system (SST)[6–8], but still they have not found a real application in large-scale recovery of LTH due to the low efficiency, high costs[9] and, more important, lack of capacities for energy storage[10,[11]. Recently, technologies based on electrochemical cells[12,13] were developed to directly convert LTH in electricity. These systems are generally based on two different concepts: the use of external thermal energy to recharge the discharged electrochemical cell, (Thermally Regenerative Electrochemical Cycles, TREC[12]) or the use of temperature gradient to sustain a potential difference between the electrodes and thus generate electricity (and Thermo-Electrochemical Cells, TEC[13]).   TREC systems use different electrochemical cells whose electrode reactions have suitable thermal coefficients, [12, 14,15, Nature Communications, 10, 4151, 2019], while TEC devices are usually made by symmetric electrodes and a redox couple in the electrolyte [REF 13, 17, Science Vol. 368, Issue 6495, pp. 1091-1098]. Recently, a new TEC device has been reported, using two flow batteries [REF Energy Environ. Sci.,2018, 11, 2964] and a temperature gradient between them. TREC and TEC result less expensive, easily scalable[14] and exhibit higher energy efficiencies[12,15,16] compared to ORC and SST systems. However, these systems reach low power densities[15,17] *e.g.*, TEC show the highest power density (12 W m^{-2}) obtained at the expense of energy efficiency (η = 0.4%)[18]. Alternatively, Salinity Gradient Energy System (SGE)[19] and Thermally Regenerative

Complexation-Based Batteries (TRCB)[14] indirectly convert heat into electricity by thermal process, which re-establishes the original conditions of the devices in term of chemical substances or concentration gradient. These systems can store thermal energy in form of chemical energy and provide electrical energy when needed. SGE systems exploit the mixing free energy (ΔG_{mix}) released by the combination of two solutions of the same salt, but with a concentration difference, to produce electrical power. Examples of this application are by Pressure Retarded Osmosis (PRO)[20–23], Reverse Electrodialysis (RED)[25–27], Capacitive Mixing (CapMix)[27,28] and Mixing Entropy Batteries (BattMix)[29] technologies. The main drawbacks of PRO and RED systems are the high membrane cost, the low efficiency and the short lifetime[30] which preclude the implementation of these technologies on a large scale[31]. CapMix and BattMix seem to be a promising solution for the low-temperature heat harvesting even if they are at the early stage of their development. In particular, CapMix undergoes to self-discharge phenomena which limits the lifetime of the device[29]. BattMix still requires further improvements in material and setup: several electrodes were proposed showing different but critical issues like high overpotential, short cycle life, dissolution or side reaction[32]. One of the most recent technology proposed to convert low-temperature heat into electrical energy, is TRCB, redox-flow cell in which power generation is related to the metal-complexes formation (Cu or Ag with acetonitrile or ammonia). The solutions are then regenerated by distillation of ammonia or acetonitrile[33–36].

TRCBs have several advantages like a simple and easily scalable setup and need relatively inexpensive reactants and electrode materials[14]. However, TRCBs exploit much smaller temperature differences compared to the other technologies here reported, resulting in lower thermal-energy efficiency[37,38]. Recently, we proposed a new concept of LTH converter, which combines elements of SGE and TRCB: the so-called Thermally Regenerable Redox-Flow Battery (TRB). It consists in a redox-flow concentration cell, producing electrical energy at the expenses of mixing free energy (ΔG_{mix}) of two water solutions at different concentration of NaI[39]. In the concentrated compartment (H), the oxidation of iodide to iodine takes place while, in the diluted compartment (L), the opposite reaction happens, resulting in the movement of sodium ions from the concentrated to diluted side of the cell through a selective cation-exchange membrane. The iodine activity is kept constant using a specifically designed "Trough-Liquid Exchanger" (TLE). When the two solutions reach the same concentration, they can be regenerated by under vacuum distillation[40] at low temperature to exploit LTH. NaI/I_2 couple has been chosen because the high boiling point elevation, which implies high distillation efficiency[41,42]. The device reaches an overall efficiency (considering the electrochemical and the thermal efficiency) close to 3%, and a maximum power density of 10W m^{-2}.

Hereby, we propose further improvements of this technology changing the chemical species with $LiBr/Br_2$. The overall scheme of the entire device is shown in Figure 1.
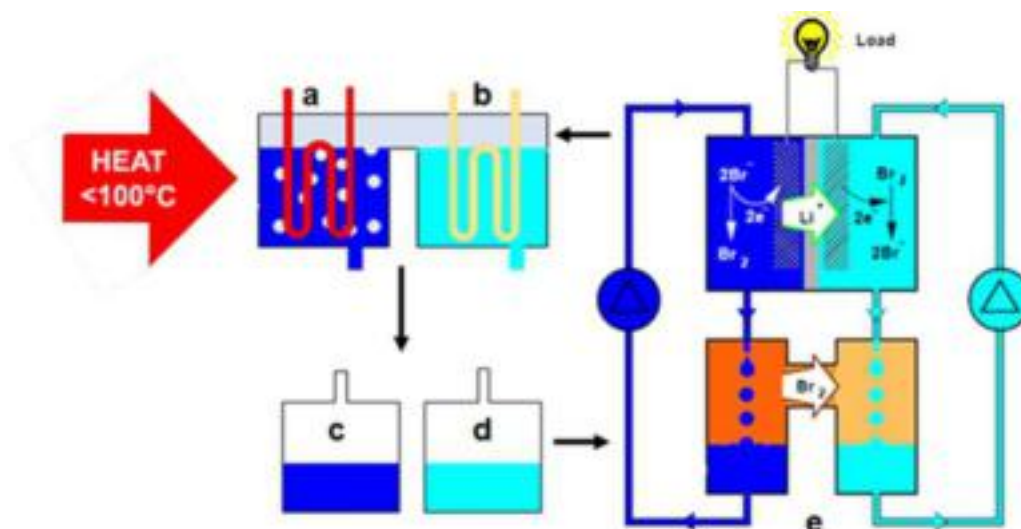
Figure 1. Scheme of the whole TRB system where a) and b) are the evaporator and condenser of the distiller; c) and d) represents the reservoirs where the fresh solutions are collected; e) is the electrochemical cell combined with the so called "Through-liquid exchanger" device. The operating temperatures are a = 85°C; b = 40°C; c and d = 25°c; e = 50°C.

LTH is used to distill the exhausted LiBr solutions (Figure 1, a) to obtain a concentrated LiBr solution (H solution) and pure water (Figure 1, b). The diluted solution (L) is then obtained by mixing a small amount of H solution with water. The H and L solutions, are stored in reservoirs (Figure 1,c and d) and then injected in the electrochemical cell (Figure 1e, top part) to convert their mixing free energy in electrical energy: in the H compartment the bromide is oxidized to bromine, while, in the other side of the cell, the opposite reaction takes place. In order to recirculate bromine from the H solution, where it is produced, to the L solution, where it is consumed, a special glassware is connected to the cell: the so called, "Trough- liquid exchanger" (TLE, Figure 1e, bottom part). The total heat-to-electricity efficiency of TRB is the product of the distillation efficiency (η_{dis}) and the efficiency of the electrochemical cell (η_{el}):

$$\eta = \eta_{el} \cdot \eta_{dis} \qquad (1)$$

The new redox couple, LiBr/Br$_2$ requires a different setup: in particular, the electrochemical cell was completely re-designed and the shape of the TLE was modified in order to achieve more efficient performances in terms of bromine equilibration time. We tested two diaphragms with different thickness by electrochemical impedance spectroscopy, evaluating the best operational conditions. Linear Sweep Voltammetry (LSV) and Galvanostatic Cycling with Potential Limitation (GCPL) were performed to assess the maximum power density/current density of the device and the behavior of the system during the discharge process.

Thanks to LiBr/Br$_2$ redox couple and the setup improvement, the device presented in this work can store more energy and recover LTH in a more efficient way than the analogue based on NaI/I$_2$ redox couple. The thermal energy harvesting and the electrochemical performances of the device are then discussed.

Results and Discussion

Distillation efficiency

Vacuum distillation technology is proposed to restore the salinity gradient of the two solutions: its lower internal pressure allows boiling at low temperature, exploiting LTH. The exhausted solution is sent from the electrochemical cell to the distiller where it boils and concentrates in contact with a heat exchanger, while its vapor is condensed in contact with a second heat exchanger. Each evaporation and condensation chambers are called "effect".

In the case of the LiBr solutions, the scheme of the distiller is particularly simple, being composed by a "single effect".

In the distiller, air is evacuated from the system, so that the pressure stabilizes to the vapor pressure of water at the temperature of the condenser, much lower than 1 atm. No external work is needed to keep the vacuum. A pressure exchanger decouples the cell from the distiller, so that the cell can be operated at 1 atm without requiring external work.

The distiller is kept at 85°C, which will be slightly less than the boiling temperature of the concentrated solution, with the exception of the condenser, kept at 40°C (85°C-40°C = 45 K, i.e. the boiling point elevation). Moreover, the electrochemical cell is kept at 50°C: this is beneficial for the conductivity of the ceramic membrane. This scheme is particularly efficient: the heat consumption is exactly equal to the latent heat needed for the evaporation of water plus the sensible heat needed to heat again the distilled water after condensation which is so small that it can be neglected. The electrochemical cell does not consume heat (the reaction is slightly exothermic).

Starting from a simplified model of vacuum distiller and heat exchanger[41–44], the evaluation of a single-effect distiller efficiency is reported hereafter.

The distillation efficiency is defined as:

$$\eta_{dis} = \frac{\Delta Gmix}{Q_H} = \frac{n_W \lambda \cdot (1 - \frac{T_W}{T_S})}{n_W \lambda} \tag{2}$$

where Q_H is the absorbed heat from the heat sources, n_W, the moles of solvent that must evaporate; λ is the latent heat of evaporation; T_W is the boiling point of pure water; T_S is the boiling point of the exhausted solution and ΔG_{mix} is the mixing free energy of the two initial solutions and it is determined as a difference between the Gibbs free energy of the exhausted

solution (G_f) and the sum of the Gibbs free energy of the H and L solutions, as reported in equation 3. The ΔG_{mix} represents the maximum energy that can be obtained if the electrochemical process was ideal and reversible:

$$\Delta G_{mix} = G_f - G_i = n_{tot}\mu_f - (n_H \mu_H + n_L \mu_L) \tag{3}$$

To increase the efficiency of the heat conversion, thermodynamic analysis evidences the importance to increase the boiling point elevation of the implemented solutions compared to the pure solvent[43,44] (Figure 2a) as it is reported in equation (2).

Moreover, from equation (2) it can be concluded that a solvent with a large latent heat of evaporation leads to an increasing of the mixing free energy even if it also corresponds to an increase of the thermal energy consumption from the heat source.

The efficiency of the single-effect distiller is defined as:

$$\eta_{eff} = \frac{\Delta G_{mix}}{Q_{H,eff}} \tag{4}$$

where $Q_{H,eff}$ is the absorbed heat from the heat sources. Distillation efficiency is limited by the Carnot law[44]:

$$\eta_d \leq 1 - \frac{T_L}{T_H} \tag{5}$$

Where T_L is the temperature of the sink, which must be lower or equal to T_W and T_H is the temperature of the heat source, which has to be higher or equal to T_S. Equation (5) can be rewrite for the single-effect distiller as follow:

$$\eta_{eff} \leq \frac{BPE}{BPE + T_{L,eff}} \tag{6}$$

Where $T_{L,eff}$ is the temperature of the condensing solvent while *BPE* is the boiling point elevation of the solution at the end of the evaporation process ($BPE = T_s - T_w$). In the working condition, the aqueous solution of lithium bromide shows a *BPE* of 45°K resulting in a distillation efficiency of 13% (Figure 2a).
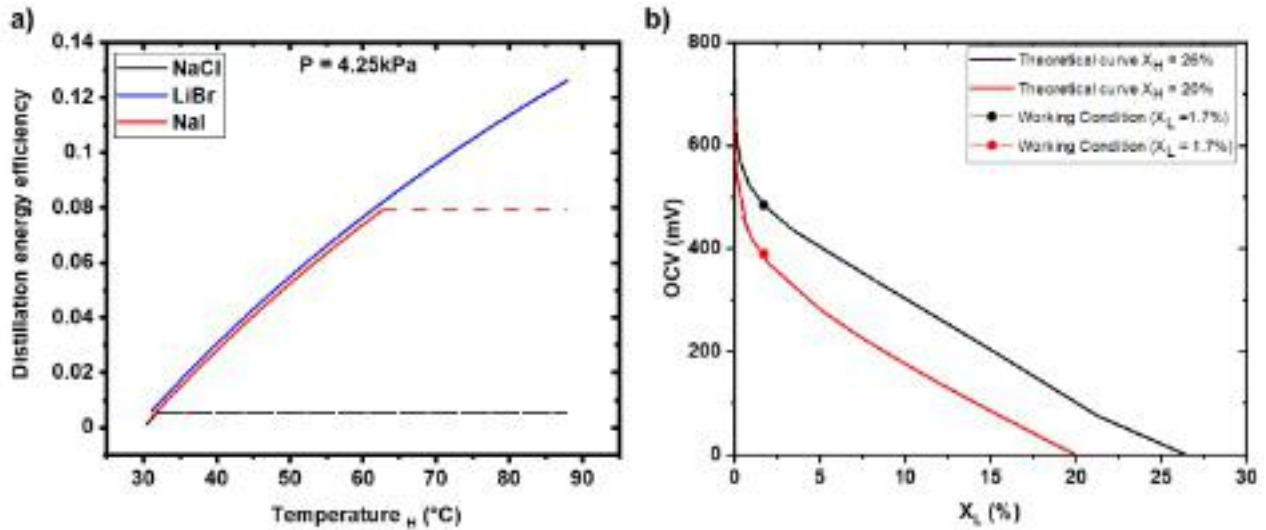
Figure.2 a) Distillation energy efficiency at the increasing of heat temperature for NaCl, LiBr and NaI water solutions. The distillation takes place at 4.25 kPa: at this pressure, pure water evaporates at 30°C. Dashed lines represent the evaporation of the solution: from the boiling point, even if the heat temperature is increased, no improvements of the distillation efficiency can be observed. **b)** Open circuit voltage of the cell vs molar fraction of L solution at fixed molar fraction of H solution (26% black curve, 20% red curve) obtained by thermodynamic analysis. The black and red dots represent experimental conditions of this work.

Considering an output power of 1kW as target, and a heat transfer coefficient U of the heat exchanger of 500W m^{-2} K^{-1} the surface of heat exchangers and the dimension of the distiller can be evaluated. Any heat exchanger, one for the evaporation of the solution and one for the condensation of its vapor, requires a surface of 3.5 m^2 when the temperature difference across the heat exchanger is 15°K, a feasible value for realistic conditions (100°C-85°C=15K, 40°C-25°C=15K) . This means the heat exchangers may be easily contained in sink of nearly 20L of volume.

Electrochemical cell

The efficiency of the electrochemical unit is:

$$\eta_{el} = \frac{W}{\Delta G_{mix}} \qquad (7)$$

Where W is the extracted work from the cell and ΔG_{mix} can be calculated by equation 3. To increase the mixing free energy that can be stored/extracted by the electrochemical cell, and the voltage of the cell (which it will be discuss later in this section) it

is necessary choose two solution with a higher concentration difference as shown in Figure 2b.

Therefore, we decided to test a TRB based on water solutions of lithium bromide using concentrated (H) and diluted (L) solutions with molar fraction of X_H = 20% (H$_{20}$) and X_L = 1.7% (L$_{1.7}$, Figure 2b). Under these conditions, the maximum energy (ΔG_{mix}) that can be extract is 16.0 Wh dm^{-3} [45]. Increasing the molar fraction of H solution to X_H = 26% (H$_{26}$) increases the available energy to 25.5 Wh dm^{-3} [45] but the salt precipitation may occur if the set-up temperature is not well-controlled.

In order to have a redox equilibrium, 2x10^{-2} mol dm^{-3} of bromine is dissolved in both solutions. When the circuit is closed, a spontaneous redox reaction takes place: bromide is oxidized to bromine in the H compartment, the concentrated one, while bromine is reduced to bromide in the L compartment, the diluted side.

$$H: \quad Br^- + e^- \rightarrow \frac{1}{2} Br_2$$

$$L: \quad \frac{1}{2} Br_2 \rightarrow Br^- + e^-$$
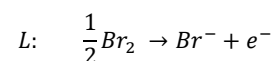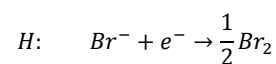
FULL PAPER

To maintain the electroneutrality, lithium ions move from the concentrated side to the diluted one through the selective cation-exchange membrane (LICGC™).

Since the solubility of bromine is minor than the solubility of lithium bromide, to avoid the power-down of the cell, it is important maintain the bromine activity in equilibrium between the H and L compartments. This is possible thank to the "Through-liquid exchanger" device, widely discussed in the next section and in the SI. Therefore, the open circuit voltage of the cell does not depend on the activity of iodine, but it is determined by the simple Nernst equation as follow:

$$OCV = \frac{RT}{F} ln \left[\frac{(X_{LiBr}^{H} \gamma_{LiBr}^{H})^2}{(X_{LiBr}^{L} \gamma_{LiBr}^{L})^2} \right] \qquad (8)$$

The electrochemical cell (Figure 3) is composed by two platinum meshes as electrodes (surface area of 3.92 cm^2) separated by a commercial solid-state electrolyte (LICGC™ diaphragm), a cation-exchange membrane which allows the passage of lithium ions but it avoids the transit of bromide, bromine and water. Two diaphragms with different thickness, 150µm and 50µm respectively, are testing. The thinner diaphragm decreases the ohmic drop because its lower resistance, which could be further decreases by operating at higher temperature, as already reported in other works[37,39] on TRB and TRCB systems. This is the reason why all the measurements are performed at 50°C by placing the cell in a bath of hot oil. Two Viton® gaskets are placed to avoid the fracture of LICGC™ plate and seal the system. The resulting exposed area of the diaphragm is 3.14 cm^2. All these parts have kept together by two PTFE plates. A platinum wire, in contact with the electrode, is used as electrical contact, passing through the PTFE plate, through a small hole. The H and L solutions are injected in the electrochemical cell from the bottom, and leave the cell from the top, passing through other two holes on the PTFE plates.
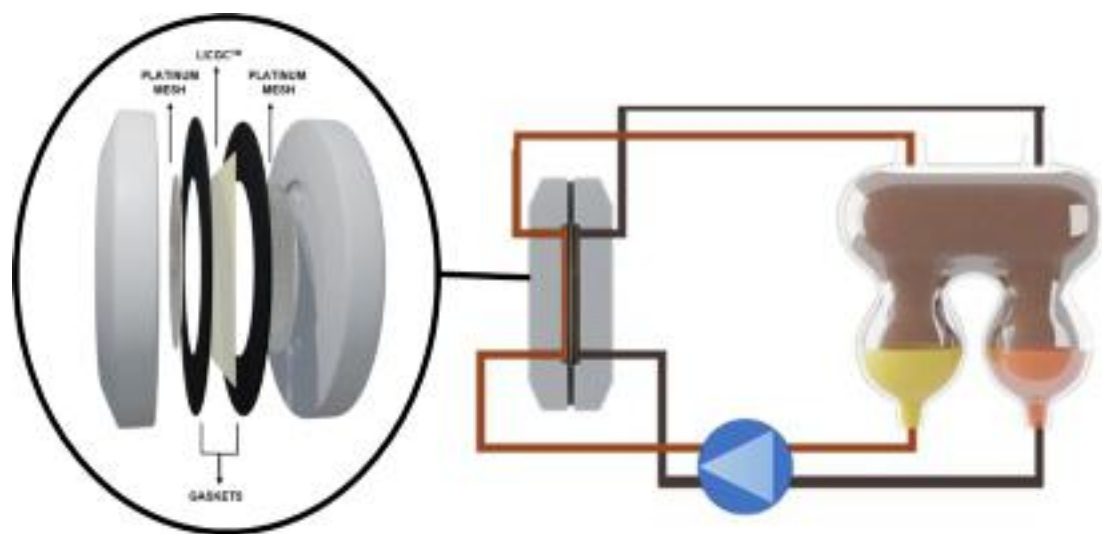
Figure 3. Scheme of the hydraulic circuit of the electrochemical part of TRB composed by the electrochemical cell and TLE. In the oval-shaped, a zoom in of the electrochemical cell is reported, to show its components.

The internal volume for any half cells is 0.628 mL. Furthermore, a new shape of "through liquid exchanger" (TLE-2; Figure 3) is tested and implemented during the electrochemical characterizations here reported (see SI from S1 to S6).

As described in the previous work[39], TLE is a glassware used to maintain the same activity of the halogen in all the system, recirculating it from the H compartment, in which is produced by oxidation of the halide, to the L compartment, where it is consumed by its reduction to halide. TLE is based on the principle

of the "liquid-liquid extraction": the two water solutions are directly in contact with an organic phase that fills the TLE: the organic solvent dissolves bromine but, at the same time, does not dissolve lithium ions, bromide ions nor water. The two water solutions, H and L, are dropped from the top of the TLE and drawn from the bottom. During the drop pathway and the contact time of the water solution with the organic one, bromine diffuses from one phase to the others until its activity is in equilibrium.

In this work, TLE is filled with octane as organic solvent, instead of toluene: this choice is related to the lower operating temperature used to conduct all the experiments. Decreasing the temperature, the water solubility in the octane also decreases, reducing the energy losses related to the mixing of the two water solutions. For this reason, the TLE operates at room temperature. The cell discharge without the implementation of TLE lasts few minutes because of the fast consumption of bromine in the diluted solution, which undergoes to reduction to bromide (Figure 4).
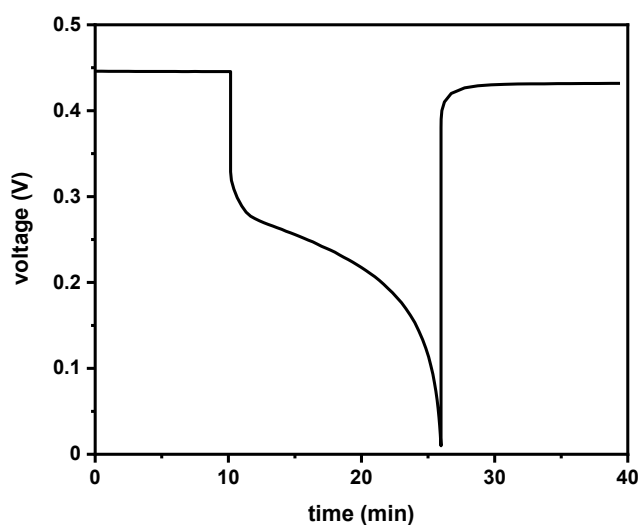
Figure 4. Discharge of the cell under constant current of 1.6 mA cm^{-2}, without the implementation of the through-liquid exchanger. The open circuit voltage is measured for the first 10 minutes, after that, the current is switched on and the voltage decreased rapidly due to the ohmic drop. After only 16 minutes the cell reaches 0 V due to the low concentration of bromine in the diluted compartment, where it is consumed undergoing a reduction reaction.

Without TLE, there is not possibility to recirculate the bromine produced in the H compartment (by the oxidation of bromide)

towards the L compartment, where it is consumed. Therefore, the TRB gives energy until all the bromine dissolved in the L solution is completely consumed.

Power density and Discharge profile

Two different couples of aqueous solutions of LiBr are used for the electrochemical characterizations. The LSV analysis is performed using H_{26} and $L_{1.7}$ as concentrated and diluted solutions, respectively. Since the concentrated solution, H_{26}, is closed to the LiBr solubility limit at room temperature (RT), for the longer discharge measurements its concentration is lowered to H_{20}, avoiding issues of salt precipitation in the TLE, during cell preparation and handling. Using eq. 8, the open circuit voltage for the solutions $H_{20}/L_{1.7}$ is 0.383 V, at room temperature; while $H_{26}/L_{1.7}$ is 0.481 V (see also Figure 2b).

The electrochemical performances of the cell, in terms of maximum current/power density, were evaluated by LSV in the range between the open circuit voltage and the 0 V, applying a scan rate of 1 mV s^{-1}. Figure 5a shows the current potential profile for the TRBs filled with $H_{26}/L_{1.7}$ solutions and different diaphragms. The observed OCVs of the electrochemical cells are 0.479 V and 0.430 V for the TRB with the 150 μm and 50 μm diaphragm, respectively. The relationship between current density and voltage is linear and from the slope of the profiles is possible to calculate the total resistances of the processes which are 22 Ω and 16 Ω for the high and low thicknesses, respectively, in good agreement with the impedance values (see the Cell impedance section in SI). The maximum current density reached by the device with the 50 μm membrane is nearly 8 mA cm^{-2} in short circuit conditions.

The linear behavior of the current/potential profile determines the parabolic behavior in the power/current curve reported in Figure 5b. The peak power is approximately 8.5 W m^{-2} in the case of TRB with the thinner membrane, and this value is achieved at current density of 4 mA cm^{-2}.
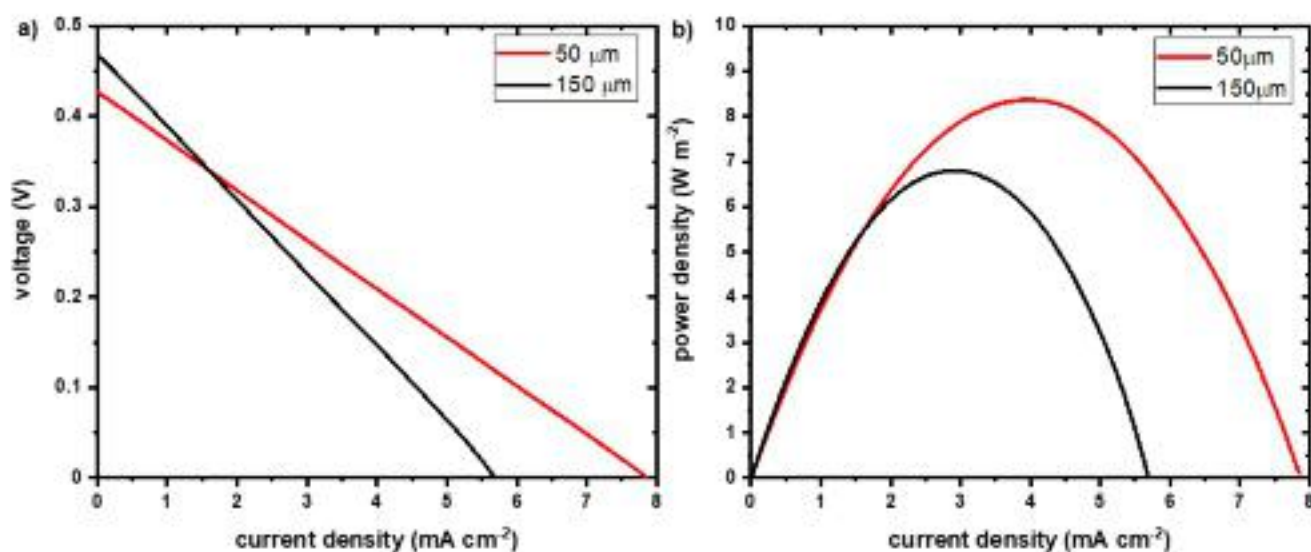
Figure 5. a) LSV between OCV and 0V of TRB based 150μm thick membrane (black curve) and TRB based on 50μm thick membrane (red curve), respectively; **b)** Power density vs current density of TRBs achieved during the LSV discharge.
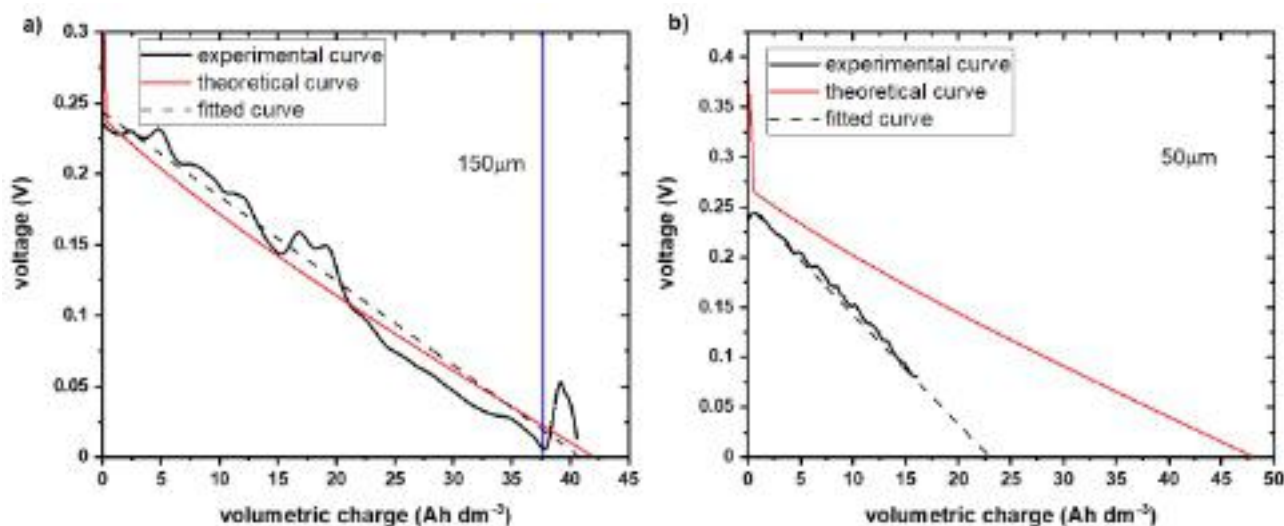
Figure 6. Discharge profiles of a) TRB with 150μm membrane, under a constant current of 1.6 mA cm^{-2} (on the left of the blue line) and 0.3mA cm^{-2} (on the right of the blue line); b) TRB with 50μm membrane under a constant current of 3.2 mA cm^{-2}. The black-solid curves represent the experimental data, the dashed lines are the fitted curves while the red profiles are the theoretical discharges (the maximum one).

The discharging profiles of a cell filled with $H_{20}/L_{1.7}$ solutions are reported in Figure 6. During the discharge under a constant current, the voltage decreases almost linearly because the non-ideality of the solutions: in the operating conditions, the chemical potential of LiBr in both H and L solutions, linearly depends on the concentration of the species.

There are small variations of the voltage connected to the temperature fluctuations and the change in the internal resistances during the electrochemical process. In particular, the resistance fluctuations are related to the charge transfer and mass transport processes, and are not connected to the diaphragm, which always shows the same resistance throughout the whole discharge process (Figure S7, S8). In general, the fluctuations are affecting the internal resistance for less than 10%. The TRB based on the thicker diaphragm is completely discharged under a constant current of 1.6 mA cm^{-2} for ≈ 62 hours

(Figure 6a). Once the potential reaches almost 0 V, the current is decreased to 0.3 mA cm^{-2} in order to reduce the ohmic losses and extract further energy (Figure 6a, on the right of the blue line). In fact, after the discharge at higher current, the LiBr concentration in the H and L solutions is not the same, but the voltage reached the 0 V value due to the ohmic loss that reduces the available energy. In these conditions, the cell was able to deliver 4.9 Wh dm^{-3}, The corresponding energy efficiency is thus 30.3% as calculated by equation 7. The energy loss is due to the effect of both the charge transfer resistance and the ohmic drop dominated by the ceramic membrane resistance (see Figure S7 and S8 and discussion thereof). We have to point out, however, that the discharge was made at practical current density (1.6 mA cm^{-2}), while higher efficiencies could be obtained at lower currents but at longer times.

The discharge of the TRB with the thinner diaphragm (Figure 6b, black-solid profile) is incomplete: unfortunately, the brittleness of the thinner diaphragm, makes hardly possible its implementation in a laboratory scale. In this case, the total extracted energy is ≈ 2.7 Wh dm^{-3} which translates in a lower efficiency of 17%. If the discharge process was complete (dashed line in Figure 6b), it would be obtained 3.1 Wh dm^{-3}, thus an electrochemical efficiency of 19%. The theoretical maximum efficiency under these operational conditions (3.2 mA cm^{-2} as applied constant current and considering an internal constant resistance of 12 Ω) would be around 38% (Figure 6b, red profile). The reason why experimentally TRB based on the thinner membrane gives only half of the maximum available energy, is related to the membrane, which broke down after only 22 hours. Probably, the rupture process was not instantaneous but a progressive degradation which brought to a slow progressive mixing of solution before the complete fragmentation.

TRB based on LiBr/Br$_2$ redox reaction is able to store more energy, in the form of mixing free energy of solutions, than TRB based on the couple NaI/I$_2$. This is possible because the higher solubility of LiBr in water, which allows to obtain more concentrated solution, and the higher activity coefficients at higher concentration, which lead to higher chemical potentials. Thus, if the maximum mixing free energy that may be exploited in a TRB based on NaI/I$_2$ couple is around 6.5 Wh dm^{-3}, in a TRB based on LiBr/Br$_2$ couple this value increases to 16.0 and 25.5 Wh dm^{-3} using H$_{26}$/L$_{1.7}$ and H$_{20}$/L$_{1.7}$ solutions, respectively. In the best conditions (H$_{20}$/L$_{1.7}$, thicker membrane), the LiBr based TRB was able to deliver 4.85 Wh dm^{-3} at 1.6 mA cm^{-2}, with an electrochemical efficiency of 30.3%. Furthermore, the distillation process that recharges the battery, exploiting low-temperature heat, is more efficient (≈13%) due to the higher boiling point elevation of LiBr. Calculating the heat-to-electricity efficiency for TRB based on the thicker diaphragm (Equation 1), the result is nearly 4%, a very high value in the field of harvesting low temperature heat in a feasible device (Figure 7) and, thus TRBs based on LiBr/Br$_2$ or NaI/I$_2$ are the best compromise in terms of power density production and energy conversion efficiency.

In conclusion, we have demonstrated the proof of concept of LiBr based TRB showing its potential on lab device which can be scaled up with more performing electrolyte membranes and electrodes. In the former case, indeed, different approaches could be used, from the realization of self-standing polymer/ceramic composites to supported systems. The electrode optimization might be a more severe issue, since the Br$_2$/Br$^-$ couple requires an electrocatalytic system to be efficient. This is a less investigated field, however the use of supported nanoparticles can greatly reduce the noble metal load as in the case of Fuel Cells or Dye Sensitized Solar Cells electrodes.

Conclusion

FULL PAPER
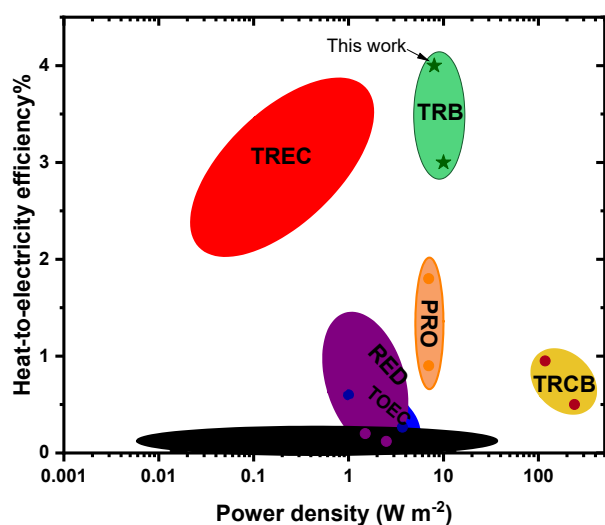
Figure 7. Heat-to-electricity efficiency vs power density of state-of-the-art technologies to harvest LTH reported in literature. Red points: Thermal Regenerative Electrochemical Cycle systems (TREC)[12,15,46]; Black points: Thermal Electrochemical Cell devices (TEC)[18,47,48]; Blue points: Thermo-Osmotic Energy Conversion technologies (TOEC)[49,50]; Orange points: Pressure Retarded Osmosis systems (PRO)[2,20,51]; Purple points: Reverse Electrodialysis Devices (RED)[25,38,52,53], Brown points: TRCBs[37,54]; Green stars: TRBs[39].

Experimental Section

Materials

Platinum meshes (52 mesh woven from 0.1mm diameter wire, 99.9%, Alfa Aesar) are used as electrodes. Platinum wires (diameter = 0.35mm) are used as electrical contacts. Gaskets (Viton®) (thickness = 0.1mm). LiBr (anhydrous, 99%, Alfa Aesar) and Br_2 liquid (99.8%, Alfa Aesar) are used to prepare the solutions. Diaphragm of LICGCTM (AG-01 plate, $25mm^2$, thickness: 0.150mm or 0.05mm; OHARA Corporation) is used as lithium-ions conductor. Octane (98+%, Alfa Aesar) is used as organic solvent in the so-called "Through-liquid exchanger", (TLE).

Hydraulic Circuit

The hydraulic circuit (Figure 3) consists in a multichannel pump (400DM2, 120S, Watson-Marlow) which recirculates the H and L solutions from the bottom of the TLE to the bottom of the

electrochemical cell. The fluxes that coming out from the top of the electrochemical cell, are then dropped in the TLE from the top, closing the cycle. All the tubes are made of marprene (Watson-Marlow) with an internal diameter of 0.23mm and 0.8mm thick. The total volume (TLE, tubes and electrochemical cell) is 8mL: 4mL for each solution. The flux is 0.8mL/min.

A solution of 20mM of Br_2 in octane fills the TLE. The halogen is added to reach the equilibrium in TLE in short time.

All the experiments are performed in a dark room to avoid radical formation of bromine using a VSP 300 Biologic potentiostat/galvanostat.

[1]   C. Forman, I. K. Muritala, R. Pardemann, B. Meyer, *Renew. Sustain. Energy Rev.* **2016**, *57*, 1568–1579.

[2]   M. Rahimi, A. P. Straub, F. Zhang, X. Zhu, M. Elimelech, C. A. Gorski, B. E. Logan, *Energy Environ. Sci.* **2018**, *11*, 276–285.

[3]   M. Pavlas, M. Tou, L. Bébar, P. Stehlík, *Appl. Therm. Eng.* **2010**, *30*, 2326–2332.

[4]   I. Dincer, *Energy Policy* **1999**, *27*, 845–854.

[5]   H. Chen, D. Y. Goswami, E. K. Stefanakos, *Renew. Sustain. Energy Rev.* **2010**, *14*, 3059–3067.

[6]   J. He, T. M. Tritt, *Science (80-.).* **2017**, *357*, DOI 10.1126/science.aak9997.

[7]   M. Saufi Sulaiman, B. Singh, W. A. N. W. Mohamed, *Energy* **2019**, 628–646.

[8]   L. Jing, P. Gang, J. Jie, *Appl. Energy* **2010**, *87*, 3355–3365.

[9] F. Vélez, J. J. Segovia, M. C. Martín, G. Antolín, F. Chejne, A. Quijano, *Renew. Sustain. Energy Rev.* **2012**, *16*, 4175–4189.

[10] L. E. Bell, *Science (80-.).* **2008**, *321*, 1457–1461.

[11] M. Zebarjadi, K. Esfarjani, M. S. Dresselhaus, Z. F. Ren, G. Chen, *Energy Environ. Sci.* **2012**, *5*, 5147–5162.

[12] Y. Yang, S. W. Lee, H. Ghasemi, J. Loomis, X. Li, D. Kraemer, G. Zheng, Y. Cui, G. Chen, *Proc. Natl. Acad. Sci. U. S. A.* **2014**, *111*, 17011–17016.

[13] M. F. Dupont, D. R. MacFarlane, J. M. Pringle, *Chem. Commun.* **2017**, *53*, 6288–6302.

[14] F. Zhang, J. Liu, W. Yang, B. E. Logan, *Energy Environ. Sci.* **2015**, *8*, 343–349.

[15] S. W. Lee, Y. Yang, H. W. Lee, H. Ghasemi, D. Kraemer, G. Chen, Y. Cui, *Nat. Commun.* **2014**, *5*, 1–6.

[16] H. Im, T. Kim, H. Song, J. Choi, J. S. Park, R. Ovalle-Robles, H. D. Yang, K. D. Kihm, R. H. Baughman, H. H. Lee, T. J. Kang, Y. H. Kim, *Nat. Commun.* **2016**, *7*, 1–9.

[17] A. P. Straub, N. Y. Yip, S. Lin, J. Lee, M. Elimelech, *Nat. Energy* **2016**, *1*, DOI 10.1038/nenergy.2016.90.

[18] L. Zhang, T. Kim, N. Li, T. J. Kang, J. Chen, J. M. Pringle, M. Zhang, A. H. Kazim, S. Fang, C. Haines, D. Al-Masri, B. A. Cola, J. M. Razal, J. Di, S. Beirne, D. R. MacFarlane, A. Gonzalez-Martin, S. Mathew, Y. H. Kim, G. Wallace, R. H. Baughman, *Adv. Mater.* **2017**, *29*, 1605652.

[19] N. Y. Yip, D. Brogioli, H. V. M. Hamelers, K. Nijmeijer, *Environ. Sci. Technol.* **2016**, *50*, 12072–12094.

[20] R. L. McGinnis, J. R. McCutcheon, M. Elimelech, *J. Memb. Sci.* **2007**, *305*, 13–19.

[21] C. Boo, Y. F. Khalil, M. Elimelech, *J. Memb. Sci.* **2015**, *473*, 302–309.

[22] N. Y. Yip, D. A. Vermaas, K. Nijmeijer, M. Elimelech, *Environ. Sci. Technol.* **2014**, *48*, 4925–4936.

[23] A. P. Straub, S. Lin, M. Elimelech, *Environ. Sci. Technol.* **2014**, *48*, 12435–12444.

[24] X. Zhu, T. Kim, M. Rahimi, C. A. Gorski, B. E. Logan, *ChemSusChem* **2017**, *10*, 797–803.

[25] A. Tamburini, M. Tedesco, A. Cipollina, G. Micale, M. Ciofalo, M. Papapetrou, W. Van Baak, A. Piacentino, *Appl. Energy* **2017**, *206*, 1334–1353.

[26] X. Luo, X. Cao, Y. Mo, K. Xiao, X. Zhang, P. Liang, X. Huang, *Electrochem. commun.* **2012**, *19*, 25–28.

[27] M. C. Hatzell, M. Raju, V. J. Watson, A. G. Stack, A. C. T. Van Duin, B. E. Logan, *Environ. Sci. Technol.* **2014**, *48*, 14041–14048.

[28] D. Brogioli, *Phys. Rev. Lett.* **2009**, *103*, 31–34.

[29] F. La Mantia, M. Pasta, H. D. Deshazer, B. E. Logan, Y. Cui, *Nano Lett.* **2011**, *11*, 1810–1813.

[30] G. Han, S. Zhang, X. Li, T. S. Chung, *Prog. Polym. Sci.* **2014**, *51*, 1–27.

[31] B. E. Logan, M. Elimelech, *Nature* **2012**, *488*, 313–319.

[32] T. Kim, M. Rahimi, B. E. Logan, C. A. Gorski, *ChemSusChem* **2016**, *9*, 981–988.

[33] F. Zhang, J. Liu, W. Yang, B. E. Logan, *Energy Environ. Sci.* **2015**, *8*, 343–349.

[34] P. Peljo, D. Lloyd, N. Doan, M. Majaneva, K. Kontturi, *Phys. Chem. Chem. Phys.* **2014**, *16*, 2831–2835.

[35] X. Zhu, M. Rahimi, C. A. Gorski, B. Logan, *ChemSusChem* **2016**, *9*, 873–879.

[36] Sunny Maye, Hubert H. Girault, Pekka Peljo, *Energy Environ. Sci.* **2020**, *13*, 2191–2199.

[37] F. Zhang, N. LaBarge, W. Yang, J. Liu, B. E. Logan, *ChemSusChem* **2015**, *8*, 1043–1048.

[38] F. Giacalone, C. Olkis, G. Santori, A. Cipollina, S. Brandani, G. Micale, *Energy* **2019**, *166*, 674–689.

[39] I. Facchinetti, R. Ruffo, F. La Mantia, D. Brogioli, *Cell Reports Phys. Sci.* **2020**, *1*, 100056.

[40] D. Wirth, C. Cabassud, *Water Sci. Technol. Water Supply* **2003**, *3*, 57–66.

[41] D. Brogioli, F. La Mantia, *AIChE J.* **2019**, *65*, 980–991.

[42] D. Brogioli, F. La Mantia, N. Y. Yip, *Renew. Energy* **2019**, *133*, 1034–1045.

[43] A. Carati, M. Marino, D. Brogioli, *Energy* **2015**, *93*, 984–993.

[44] D. Brogioli, F. La Mantia, N. Y. Yip, *Desalination* **2018**, *428*, 29–39.

11

[45]   William M. Haynes., *CRC Handbook of Chemistry and Physics*, **2015**.

[46]   Y. Yang, J. Loomis, H. Ghasemi, S. W. Lee, Y. J. Wang, Y. Cui, G. Chen, *Nano Lett.* **2014**, *14*, 6578–6583.

[47]   K. Kim, H. Lee, *Phys. Chem. Chem. Phys.* **2018**, *20*, 23433–23440.

[48]   J. Duan, G. Feng, B. Yu, J. Li, M. Chen, P. Yang, J. Feng, K. Liu, J. Zhou, *Nat. Commun.* **2018**, *9*, 1–8.

[49]   Z. Zhang, S. Yang, P. Zhang, J. Zhang, G. Chen, X. Feng, *Nat. Commun.* **2019**, *10*, DOI 10.1038/s41467-019-10885-8.

[50]   A. P. Straub, M. Elimelech, *Environ. Sci. Technol.* **2017**, *51*, 12925–12937.

[51]   A. Altaee, P. Palenzuela, G. Zaragoza, A. A. AlAnezi, *Appl. Energy* **2017**, *191*, 328–345.

[52]   R. Long, B. Li, Z. Liu, W. Liu, *J. Memb. Sci.* **2017**, *525*, 107–115.

[53]   F. Giacalone, F. Vassallo, L. Griffin, M. C. Ferrari, G. Micale, F. Scargiali, A. Tamburini, A. Cipollina, *Energy Convers. Manag.* **2019**, *189*, 1–13.

[54]   W. Wang, H. Tian, G. Shu, D. Huo, F. Zhang, X. Zhu, *J. Mater. Chem. A* **2019**, *7*, 5991–6000.

FULL PAPER

Entry for the Table of Contents
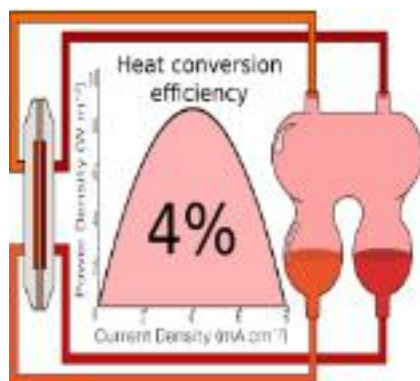
TRB based on LiBr/Br$_2$ couple is a promising redox flow cell able to produce energy at the expenses of the salinity gradient of two LiBr water solutions. Restoring the exhausted solution by means vacuum distillation, TRB harvests low-temperature heat sources (below 100°C). The system reaches high value of power density and the heat to electricity efficiency of the TRB here proposed is around 4%: the highest value reached in this field.

13

14